ELSEVIER

Journal of Photochemistry and Photobiology A: Chemistry 103 (1997) 231–237

Journal of PHOTOCHEMISTRY AND PHOTOBIOLOGY A:CHEMISTRY

Real-time Fourier transform IR (FTIR) spectroscopy in organometallic chemistry: mechanistic aspects of the fac to mer photoisomerization of *fac*-[Mn(Br)(CO)$_3$(R-DAB)]

Cornelis J. Kleverlaan, František Hartl, Derk J. Stufkens *

Anorganisch Chemisch Laboratorium, J.H. van't Hoff Research Institute, Universiteit van Amsterdam, Nieuwe Achtergracht 166, 1018 WV Amsterdam, Netherlands

Received 21 June 1996; accepted 6 August 1996

Abstract

Real-time Fourier transform IR (RT/FTIR) spectroscopy was used to study the photoisomerization of *fac*-[Mn(Br)(CO)$_3$(R-DAB)] (R-DAB, *N,N'*-di-R-1,4-diazabutadiene; R≡^{i}Pr, ^{t}Bu) to *mer*-[Mn(Br)(CO)$_3$(R-DAB)]. The primary photoproduct [Mn(Br)(L)-(CO)$_2$(R-DAB)] could be detected at room temperature for L≡MeCN and identified at 273 K as a cis–cis isomer for L≡P(OMe)$_3$. RT/FTIR spectroscopy was also used to determine the thermodynamic parameters E_a, $\Delta H^{\ddagger}$ and $\Delta S^{\ddagger}$ of the thermal backreaction of this mer product to the parent fac isomer.

For slow reactions, GC/FTIR software was used to provide a real-time screen display of the IR spectral changes. For fast reactions (10^{-1}–1 s), the high speed collect (HSC) kinetic software was used to collect 12 spectra s^{-1} at 2 cm^{-1} resolution, recording one spectrum per scan.

Keywords: α-Diimine complexes; Kinetics; Manganese carbonyls; (Photo)isomerization; Real-time FTIR spectroscopy

1. Introduction

Organometallic complexes containing an α-diimine ligand bound to a low-valent metal atom have been the subject of many photochemical and photophysical studies [1–4]. The complexes d^6-*fac*-[Re^I(L)(CO)$_3$(α-diimine)]$^{n+}$ (α-diimine≡bpy, etc.; n=0, 1) continue to attract attention because of their ability to act as efficient photosensitizers for intramolecular and intermolecular energy and electron transfer processes [5]. These complexes exhibit an intense absorption band in the visible or near-UV region which can be attributed to metal-to-ligand charge transfer (MLCT) transitions directed to the lowest π^* orbital of the α-diimine ligand. Irradiation into this MLCT band does not lead to a photoreaction. On the other hand, the corresponding Mn complexes *fac*-[Mn(X)(CO)$_3$(α-diimine)] (X≡halide; α-diimine≡bpy, pyridine-2-carbaldehyde-N-isopropylimine(^{i}Pr-Py(a)),pyridine-2-carbaldehyde–N-p-tolylimine (^{p}Tol-PyCa)) have recently been found to be photolabile and to undergo, at room temperature, the remarkable, seemingly simple, photoreaction described by Eq. (1) [6]

$$fac\text{-}[Mn(X)(CO)_3(\alpha\text{-diimine})] \xrightarrow[-X^{\cdot}]{h\nu} 1/2[Mn_2(CO)_6(\alpha\text{-diimine})_2] \quad (1)$$

The fate of X$^{\cdot}$ is unclear.

However, low-temperature IR and UV–visible measurements have shown that this reaction proceeds via several intermediates and most probably via the mechanism given in Scheme 1 [6].

According to this mechanism, the parent fac complex loses CO on irradiation with the formation of a photoproduct *cis–cis*-[Mn(X)(Sv)(CO)$_2$(α-diimine)] in which the halide X and the solvent Sv, as well as the two carbonyls, are in a cis position with respect to each other. Only one of the two possible isomers was detected. In view of the low temperature at which the photoproduct was formed (135 K), Stor et al. [6] assumed that the halide had retained its axial position and that the solvent molecule had replaced an equatorial carbonyl ligand. However, recent density functional calculations on *fac*-[Mn(Cl)(CO)$_3$(H-DAB)] showed that the release of an equatorial CO ligand is accompanied by a shift of the chloride to the open equatorial site [7]. Because of this, the second cis–cis isomer (complex **b**) has now been added as a possible primary photoproduct to Scheme 1.

* Corresponding author. Tel.: 31 20 525 6451; fax: 31 20 525 6456.

PII S1010-6030(96)04477-2

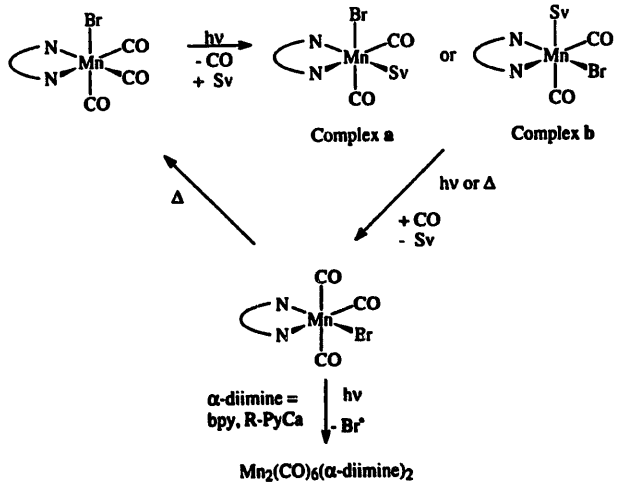

Scheme 1. Proposed mechanism of the photoreaction of *fac*-[Mn(Br)-$(CO)_3$(α-diimine)].

As mentioned above, this mechanism was mainly derived from spectroscopic data obtained for the intermediates at low temperatures. At room temperature, the dimer $[Mn_2(CO)_6(\alpha\text{-diimine})_2]$ was observed as a major product, together with a small amount of the intermediate mer isomer in the case of the bpy complex [6].

Preliminary results have shown that the corresponding α-diimine complexes *fac*-[Mn(Br)$(CO)_3$(R-DAB)] (R-DAB, *N,N'*-di-R-1,4-diazabutadiene; R ≡ ^{i}Pr, ^{t}Bu) do not produce dimers at room temperature, but photodecompose into products which could not be characterized further by conventional spectroscopic techniques. In order to determine at which stage of the reaction sequence in Scheme 1 decomposition occurs, real-time Fourier transform IR (RT/FTIR) spectroscopy in the millisecond to second time domain was used.

Up to now, only a few organometallic photoreactions [8,9] have been studied with RT/FTIR spectroscopy, and the technique has more widely been used for kinetic studies of polymerization reactions [10]. In this paper, we present the results of an RT/FTIR study on the photoreaction of *fac*-[Mn(Br)$(CO)_3$(R-DAB)]. Special attention is paid to the fac to mer photoisomerization, the molecular structure of the intermediate dicarbonyl complex and the thermal back-

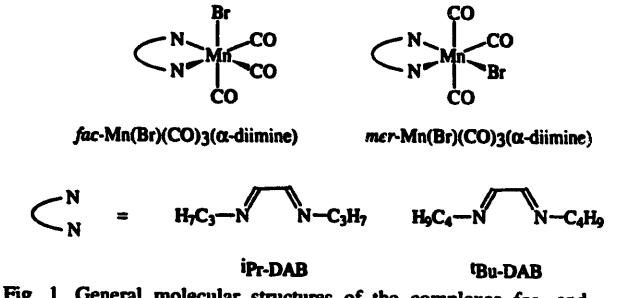

Fig. 1. General molecular structures of the complexes *fac*- and *mer*-[Mn(Br)$(CO)_3$(α-diimine)] and the α-diimine ligands used.

reaction of *mer*-[Mn(Br)$(CO)_3$(R-DAB)] to the parent fac complex (Scheme 1).

The structures of the *fac*- and *mer*-[Mn(Br)$(CO)_3$(R-DAB)] complexes and the R-DAB ligands are depicted schematically in Fig. 1.

2. Experimental details

2.1. Materials and preparations

Tetrahydrofuran (THF; Janssen) and 2-methyl-tetrahydrofuran (2-MeTHF; Janssen) were dried on sodium wire. Acetonitrile (MeCN; Janssen) was refluxed with CaH_2. The solvents were distilled under a nitrogen atmosphere prior to use. ^{i}Pr-DAB and ^{t}Bu-DAB were synthesized according to literature procedures [11]. The complexes *fac*-[Mn(Br)-$(CO)_3$(R-DAB)] (R ≡ ^{i}Pr, ^{t}Bu) were prepared as described previously [12], with the modification that the reactants were refluxed in hexane for 3 h in the absence of light. The products were purified in the dark by column chromatography on activated Silica 60 (Merck), with a gradient elution of hexane–THF. All spectroscopic samples were prepared by standard inert gas techniques and were 10^{-2} M in *fac*-[Mn(Br)-$(CO)_3$(R-DAB)].

2.2. Instrumentation and spectroscopic measurements

All RT/FTIR kinetic runs of the photochemical and thermal isomerization reactions were carried out with a Bio-Rad FTS 60A system equipped with a dual-source Digital Module 896 interferometer, a liquid-nitrogen-cooled MCT detector and KRS 5 filters in the sample compartment. To follow the fast photoisomerization of *fac*-[Mn(Br)$(CO)_3$(R-DAB)] into its mer isomer, one spectrum per scan was taken at a resolution of 2 cm^{-1}. With a detector speed of 125 kHz, the time interval between the scans (12 in total) was 83 ms (bidirectional motion). The interferograms were collected first; post-Fourier transform conversion and spectral script reduction were then performed (high speed collect (HSC)). For slower kinetic studies of the thermal isomerization (mer to fac), the response was changed to one spectrum per seven scans at 2 cm^{-1} resolution, which resulted in a time resolution of one spectrum per second (monodirectional motion). In this case, GC/FTIR software was employed which provided a real-time screen display of the IR spectral changes during the course of the reaction. The experimental set-up used is depicted schematically in Fig. 2.

Temperature control of the sample solution was achieved with an Oxford DN 1704/54 liquid-nitrogen cryostat which contained a home-built IR cell equipped with CaF_2 windows. The samples were irradiated inside the sample compartment of the spectrometer with the 488.0 nm line of a Spectra Physics 2025 Ar^+ laser. The irradiation interval was fixed by a computer-controlled mechanical shutter. Incident light intensities were measured with a Coherent model 212 power

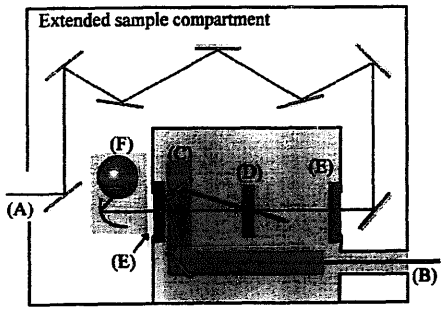

Fig. 2. Experimental set-up used for the RT/FTIR experiments: (A) IR beam; (B) laser beam; (C) optical bench with mirrors; (D) IR cell; (E) KRS 5 filters; (F) liquid-nitrogen-cooled MCT detector.

meter. The electronic absorption spectra were recorded on a Varian Cary 4E spectrophotometer.

3. Results

3.1. The fac to mer photoisomerization of fac-[Mn(Br)(CO)$_3$(R-DAB)] (R≡^{i}Pr, ^{t}Bu) in THF

The ν(CO) frequencies of the parent complexes *fac*-[Mn(Br)(CO)$_3$(R-DAB)] and their photoproducts are collected in Table 1.

Contrary to the behaviour of the corresponding bpy complex [6], continuous irradiation of *fac*-[Mn(Br)(CO)$_3$(R-DAB)] in THF into its lowest energy MLCT band ($\lambda_{max}\approx 485$ nm) does not produce the dimer [Mn$_2$(CO)$_6$(R-DAB)$_2$], but gives rise to photodecomposition. When this reaction was monitored at room temperature by conventional FTIR spectroscopy, on a timescale of 10–10^2 s, no intermediate carbonyl complex was detected in the ν(CO) region. The only product observed was free CO weakly absorbing at 2135 cm^{-1}.

The same photoreaction was then followed on a shorter timescale with RT/FTIR. For this purpose, a solution of *fac*-[Mn(Br)(CO)$_3$(R-DAB)] in THF was irradiated for 4 s with the 488.0 nm line of an Ar$^+$ laser (P=50 mW). During this period, eight spectra were measured, and the IR spectral changes for *fac*-[Mn(Br)(CO)$_3$(^{i}Pr-DAB)] are presented in Fig. 3. The irradiation results in the partial (approximately 20%) conversion of the parent complex into a product having CO stretching vibrations at 2047 (w), 1967 (s) and 1919 (m) cm^{-1} for R≡^{i}Pr and at 2046 (w), 1961 (s) and 1917 (m) cm^{-1} for R≡^{t}Bu. A similar intensity pattern of the ν(CO) bands has been reported for the complexes *mer*-[Mn(CO)$_3$(PR$_3$)(L)]$^+$ClO$_4^-$ (L≡Ph$_2$P(CH$_2$)$_n$PPh$_2$, n=1 (dppm), n=2 (dppe)) [13], *mer*-[Mn(X)(CO)$_3$(dppm)] (X≡Cl, Br) [14] and *mer*-[Mn(Br)(CO)$_3$(α-diimine)] (α-diimine≡bpy, ^{i}Pr-PyCa, ^{p}Tol-PyCa) [6]. In particular, the low intensity and large wavenumber of the highest frequency vibration are characteristic of these complexes with two carbonyl ligands in the trans position. The above product is therefore unambiguously assigned to *mer*-[Mn(Br)-(CO)$_3$(R-DAB)]. On further irradiation, this mer complex photodecomposes. Apart from free CO, no products were observed, even with RT/FTIR spectroscopy.

3.2. Detection and characterization of the intermediate dicarbonyl photoproduct

The results obtained in THF clearly show that the RT/FTIR technique, at most providing 12 spectra s^{-1}, is not fast enough to detect the solvent-substituted intermediate [Mn(Br)(THF)(CO)$_2$(R-DAB)] in the fac to mer photoisomerization. In order to be able to observe this intermediate at room temperature, the photoreaction was performed in the more strongly coordinating solvent MeCN.

The complex *fac*-[Mn(Br)(CO)$_3$(^{i}Pr-DAB)] was dissolved in MeCN and irradiated at 303 K for 2 s (P=50 mW) into its lowest MLCT band. The RT/FTIR spectra were measured simultaneously and showed the formation of a thermally unstable photoproduct with ν(CO) bands at 1941 (s) and

Table 1
ν(CO) stretching frequencies of *fac*-[Mn(Br)(CO)$_3$(R-DAB)] (R≡^{i}Pr, ^{t}Bu) and their photoproducts

Complex	Solvent	T(K)	ν(CO) (cm^{-1})
fac-[Mn(Br)(CO)$_3$(^{i}Pr-DAB)]	THF	293	2023 (s), 1938 (m), 1918 (m)
	MeCN	303	2026 (s), 1934 (m), 1926 (m)
fac-[Mn(Br)(CO)$_3$(^{t}Bu-DAB)]	THF	293	2020 (s), 1930 (m), 1917 (m)
	MeCN	303	2023 (s), 1930 (s, br)
mer-[Mn(Br)(CO)$_3$(^{i}Pr-DAB)]	THF	293	2047 (w), 1967 (s), 1919 (m)
	MeCN	303	2048 (w), 1965 (s), 1893 (m)
mer-[Mn(Br)(CO)$_3$(^{t}Bu-DAB)]	THF	293	2046 (w), 1961 (s), 1917 (m)
	MeCN	303	2035 (w), 1964 (s), 1889 (m)
[Mn(Br)(MeCN)(CO)$_2$(^{i}Pr-DAB)]	MeCN	303	1941 (s), 1866 (m)
[Mn(Br)(MeCN)(CO)$_2$(^{t}Bu-DAB)]	MeCN	303	1940 (s), 1862 (m)
[Mn(Br)(2-MeTHF)(CO)$_2$(^{i}Pr-DAB)]	2-MeTHF	135	1931 (s), 1861 (m)
[Mn{P(OMe)$_3$}$_2$(CO)$_2$(^{i}Pr-DAB)]$^+$Br$^-$	THF	293	1966 (s), 1894 (s)
	MeCN	303	1972 (s), 1901 (s)
[Mn(Br){P(OMe)$_3$}(CO)$_2$(^{i}Pr-DAB)] [a]	THF	273	1962 (s), 1875 (m)

[a] Product **b** in Scheme 1.

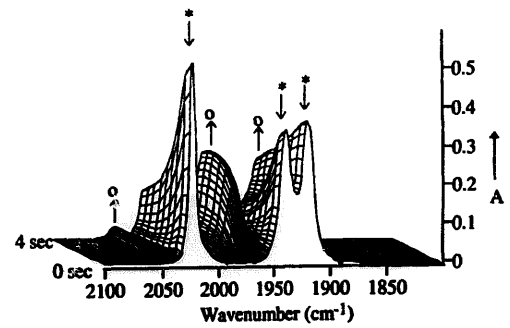

Fig. 3. IR spectral changes in the carbonyl stretching region during the photoconversion of *fac*-[Mn(Br)(CO)$_3$(ⁱPr-DAB)] (*) into *mer*-[Mn(Br)(CO)$_3$(ⁱPr-DAB)] (O) in THF at 293 K (λ_{irr}=488.0 nm; laser power, 50 mW; pulse duration, 4 s). Spectra were collected using the RT/FTIR technique (resolution, 2 cm^{-1}; scanning speed, 2 spectra s^{-1}).

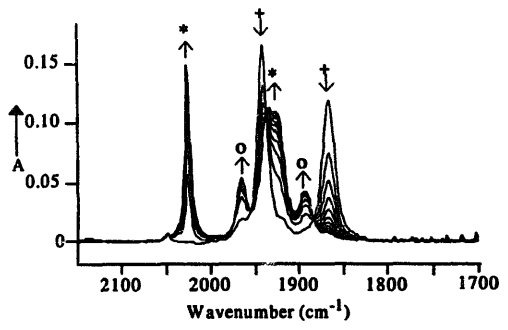

Fig. 4. IR spectral changes in the carbonyl stretching region during the thermal conversion of [Mn(Br)(MeCN)(CO)$_2$(ⁱPr-DAB)] (+) into *fac*-[Mn(Br)(CO)$_3$(ⁱPr-DAB)] (*) and *mer*-[Mn(Br)(CO)$_3$(ⁱPr-DAB)] (O) in MeCN at 303 K. Spectra were collected using the RT/FTIR technique (resolution, 2 cm^{-1}; scanning speed, 1 spectrum min^{-1}).

1866 (m) cm^{-1}. These bands are assigned to the photosubstitution product [Mn(Br)(MeCN)(CO)$_2$(ⁱPr-DAB)]. This assignment is supported by the observation that the irradiation of *fac*-[Mn(Br)(CO)$_3$(ⁱPr-DAB)] in 2-MeTHF at 135 K also results in the formation of a stable dicarbonyl complex with ν(CO) at 1931 (s) and 1861 (m) cm^{-1}. A similar photoreaction was reported for the corresponding complexes *fac*-[Mn(Br)(CO)$_3$(α-diimine)] (α-diimine ≡ bpy, ⁱPr-PyCa, ᵗTol-PyCa) under identical conditions [6]. The dicarbonyl photoproducts of the latter complexes possess ν(CO) bands between 1926 and 1921 cm^{-1} and at 1857 (s) and 1842 (m) cm^{-1} respectively. In addition, irradiation of *fac*-[Mn(Br)(CO)$_3$(ᵗTol-PyCa)] in neat pyridine at room temperature affords the stable photoproduct [Mn(Br)(pyridine)(CO)$_2$(ᵗTol-PyCa)] with ν(CO) at 1938 (s) and 1862 (s) cm^{-1} [6].

A similar dicarbonyl intermediate was obtained on irradiation of the ᵗBu-DAB derivative (Table 1). When the irradiation was stopped, approximately 70% of [Mn(Br)(MeCN)(CO)$_2$(R-DAB)] reacted back thermally to give the parent complex *fac*-[Mn(Br)(CO)$_3$(R-DAB)], while 30% was converted into the mer isomer (Fig. 4). The estimated lifetime of [Mn(Br)(MeCN)(CO)$_2$(ᵗBu-DAB)] at 303 K is approximately 15 s; for the corresponding ⁱPr-DAB complex, it is approximately 140 s.

In order to establish which isomer [Mn(Br)(MeCN)(CO)$_2$(ⁱPr-DAB)] (see Scheme 1, complex **a** or **b**) is formed, the photoreaction of *fac*-[Mn(Br)(CO)$_3$(ⁱPr-DAB)] in MeCN was also performed in the presence of excess P(OMe)$_3$ (1 : 50). Irradiation of this solution for 2 s at 303 K gives rise to the formation of [Mn(Br)(MeCN)(CO)$_2$(ⁱPr-DAB)] as the primary photoproduct. This product reacts thermally with P(OMe)$_3$ to give a species with ν(CO) bands at 1972 (s) and 1901 (s) cm^{-1}, which is assigned to the ionic complex *trans–cis*-[Mn{P(OMe)$_3$}$_2$(CO)$_2$(ⁱPr-DAB)]$^+$Br$^-$ [15]. Unfortunately, the intermediate of the reaction, [Mn(Br){P(OMe)$_3$}(CO)$_2$(ⁱPr-DAB)], formed by the substitution of MeCN by P(OMe)$_3$, could not be observed under these circumstances, even with RT/FTIR. Apparently, its transformation into stable *trans–cis*-[Mn{P(OMe)$_3$}$_2$(CO)$_2$(ⁱPr-DAB)]$^+$Br$^-$ is too fast at room temperature when excess P(OMe)$_3$ is present in solution.

In order to detect this intermediate, the photoreaction of *fac*-[Mn(Br)(CO)$_3$(ⁱPr-DAB)] with P(OMe)$_3$ was performed at 283 K in THF and monitored again with RT/FTIR. An intermediate, not formed in the absence of P(OMe)$_3$, was then observed (ν(CO) at 1962 (s) and 1875 (s) cm^{-1}). This intermediate, assigned as [Mn(Br){P(OMe)$_3$}(CO)$_2$(ⁱPr-DAB)], reacted thermally with P(OMe)$_3$ within less than 10 s to give *trans–cis*-[Mn{P(OMe)$_3$}$_2$(CO)$_2$(ⁱPr-DAB)]$^+$Br$^-$. When this photoreaction was performed at 273 K in THF, the complex [Mn(Br){P(OMe)$_3$}(CO)$_2$(ⁱPr-DAB)] remained as a stable complex with ν(CO) bands at 1962 (s) and 1875 (s) cm^{-1}. Its UV–visible spectrum showed absorption bands at 658 and 493 nm. Raising the temperature to 298 K again led to the smooth conversion of this intermediate into the stable ionic complex *trans–cis*-[Mn{P(OMe)$_3$}$_2$(CO)$_2$(ⁱPr-DAB)]$^+$Br$^-$.

3.3. The thermal mer to fac isomerization of mer-[Mn(Br)(CO)$_3$(R-DAB)] in THF

The thermal isomerization of *mer*-[Mn(Br)(CO)$_3$(R-DAB)] to give the parent complex *fac*-[Mn(Br)(CO)$_3$(R-DAB)] was investigated as follows. The initial step, i.e. the fac to mer photoisomerization of *fac*-[Mn(Br)(CO)$_3$(R-DAB)], was identical to that described above. After the irradiation period of 4 s, transient IR absorption spectra were collected within a time interval appropriate for the lifetime of the mer isomer. The resulting intensity changes of the ν(CO) bands accompanying the thermal mer to fac isomerization of *mer*-[Mn(Br)(CO)$_3$(ⁱPr-DAB)] are depicted as transient IR absorption spectra in Fig. 5.

The intensity of the ν(CO) band of the *mer*-[Mn(Br)(CO)$_3$(ⁱPr-DAB)] complex at 1967 cm^{-1} was monitored as a function of time. A linear correlation was found between the logarithm of the intensity of this band and the reaction time, which means that the thermal isomerization reaction proceeds according to (pseudo)first-order kinetics

Table 2
Lifetime (s) [a] of *mer*-[Mn(Br)(CO)$_3$(R-DAB)] (R≡^{i}Pr, ^{t}Bu) in THF at different temperatures (K) [b]

Complex	Lifetime (s)				
	293 K	288 K	283 K	278 K	273 K
R≡^{i}Pr	33.9 (1.3)	74.4 (0.2)	149.9 (1.8)	283.1 (10.2)	544.6 (3.5)
R≡^{t}Bu	1.2 (1.2)	2.3 (5.2)	4.6 (5.9)	8.7 (2.5)	17.4 (0.1)

[a] Standard deviation (%) in parentheses.
[b] $T\pm0.1$ K.

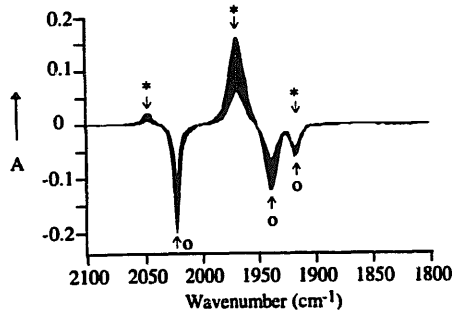

Fig. 5. Transient IR spectral changes in the carbonyl stretching region during the thermal isomerization of *mer*-[Mn(Br)(CO)$_3$(^{i}Pr-DAB)] (*) to *fac*-[Mn(Br)(CO)$_3$(^{i}Pr-DAB)] (O) in THF at 293 K. Spectra were collected using the RT/FTIR technique (resolution, 2 cm^{-1}; scanning speed, 1 spectrum every 2 s).

Table 3
Activation parameters [a,b] for the formation of *fac*-[Mn(Br)(CO)$_3$(R-DAB)] (R≡^{i}Pr, ^{t}Bu) from *mer*-[Mn(Br)(CO)$_3$(R-DAB)]

R-DAB	E_a	$\Delta H^{\ddagger}$	$\Delta S^{\ddagger}$
^{i}Pr-DAB	91.4±6.8	89.1±6.8	29±24
^{t}Bu-DAB	88.8±1.6	86.5±1.6	49±6

[a] E_a and $\Delta H^{\ddagger}$ in kJ mol^{-1}; $\Delta S^{\ddagger}$ in J mol^{-1} K^{-1}.
[b] Error based on 95% confidence interval.

(Eq. (2)). A very similar behaviour was found for the corresponding ^{t}Bu-DAB complex (see Table 2).

The reaction rates of the thermal isomerization of the two *mer*-[Mn(Br)(CO)$_3$(R-DAB)] (R≡^{i}Pr, ^{t}Bu) complexes were found to decrease rapidly with decreasing temperature. The lifetimes (τ) of the mer isomers at different temperatures are listed in Table 2.

$$[\text{mer}]_t = [\text{mer}]_0 e^{-kt} \text{ and } \tau = k^{-1} \quad (2)$$

$$k = Ae^{-E_a/RT} \quad (3)$$

$$k = Be^{\Delta S^{\ddagger}/R} e^{-\Delta H^{\ddagger}/RT} \quad (4)$$

By determining τ and hence the (pseudo)first-order rate constants k (Eq. (2)), the activation parameters of the reaction can be calculated. The Arrhenius equation (Eq. (3)) was used to calculate the activation energy E_a, and the Eyring equation (Eq. (4)) was used to determine the entropy (the errors in the entropy, based on a 95% confidence interval, are in the range 6–24 J mol^{-1} K^{-1}; this relatively large error is due to the small temperature range observed) and enthalpy of activation, $\Delta S^{\ddagger}$ and $\Delta H^{\ddagger}$ respectively. These activation parameters are collected in Table 3.

4. Discussion

In the previous section, we presented the results of an RT/FTIR spectroscopic study of the photoisomerization of *fac*-[Mn(Br)(CO)$_3$(R-DAB)] at room temperature. The use of this technique with a time resolution of 83 ms was necessary, since conventional IR spectra only show the photodecomposition of these complexes. RT/FTIR spectroscopy fills the gap between nanosecond to microsecond time-resolved and conventional IR spectroscopy. The former technique has been very successful in the characterization of primary photoproducts and excited states of transition metal carbonyls [16]. Rapid scan RT/FTIR spectroscopy, on the other hand, is particularly useful for the characterization of long-lived intermediates. The results of this study show the advantages and limitations of this technique, which will now be discussed in more detail.

It has been shown [6] that the irradiation of *fac*-[Mn(Br)(CO)$_3$(bpy)] leads to the formation of [Mn$_2$(CO)$_6$(bpy)$_2$] (Eq. (1)) and that this reaction proceeds via the intermediates shown in Scheme 1. At room temperature, only the intermediate mer isomer and the final dimeric product can be detected, and the complete mechanism can only be established by performing this photoreaction at sufficiently low temperatures.

For the corresponding *fac*-[Mn(Br)(CO)$_3$(R-DAB)] complexes, photodecomposition is too fast to be followed by conventional IR spectroscopy. However, with the use of RT/FTIR spectroscopy, the intermediate *mer*-[Mn(Br)-(CO)$_3$(R-DAB)] complexes can be observed, and photodecomposition appears to occur on irradiation of these compounds. Unfortunately, the course of the photodecomposition cannot be established with RT/FTIR spectroscopy.

Although the mer isomer can be observed with RT/FTIR spectroscopy, the primary photoproduct, i.e. the solvent-substituted dicarbonyl product (Scheme 1), is still too short lived in THF to be detected at room temperature. However, when MeCN is used as solvent, the dicarbonyl product [Mn(Br)(MeCN)(CO)$_2$(R-DAB)] has a much longer lifetime (approximately 15 s for R≡^{t}Bu and approximately 140 s for R≡^{i}Pr) and its photogeneration can easily be mon-

itored by RT/FTIR spectroscopy. Another dicarbonyl derivative, namely [Mn(Br){P(OMe)$_3$}(CO)$_2$(^{i}Pr-DAB)] is observed with RT/FTIR spectroscopy as a short-lived species ($\tau < 10$ s) on irradiation of *fac*-[Mn(Br)(CO)$_3$(R-DAB)] in THF in the presence of excess P(OMe)$_3$ at 283 K. This complex is completely stable at 273 K.

For both *fac*-[Mn(Br)(CO)$_3$(R-DAB)] complexes, only one of the four possible isomers of the dicarbonyl product is formed. The same result has been obtained on irradiation of *fac*-[Mn(Br)(CO)$_3$(α-diimine)] (α-diimine ≡ bpy, ^{i}Pr-PyCa, ^{n}Tol-PyCa) in 2-MeTHF at 135 K [6]. As mentioned in Section 1, no convincing evidence can be provided in the latter case for the formation of either complex **a** or **b** (Scheme 1). Isomer **a** is proposed to be the most probable candidate since concomitant loss of CO and site exchange of the halide are considered to be rather improbable at such a low temperature. However, recent density functional calculations of *fac*-[Mn(Cl)(CO)$_3$(H-DAB)] have shown that such a process probably occurs on release of an equatorial CO ligand [7].

Our RT/FTIR data do not allow us to distinguish between isomer **a** and **b**, since both isomers may have very similar CO stretching frequencies. However, important information is provided by the UV–visible absorption spectrum of [Mn(Br){P(OMe)$_3$}(CO)$_2$(^{i}Pr-DAB)]. The lowest energy band of this complex at 658 nm is strongly red shifted with respect to that of the parent complex *fac*-[Mn(Br)-(CO)$_3$(^{i}Pr-DAB)] (λ_{max} = 485 nm). In the case of *fac*-[Mn(Br)(CO)$_3$(bpy)], a comparable shift of λ_{max} has been observed on irradiation of the complex in 2-MeTHF at 135 K (430→630 nm) [6]. In the latter case, this shift may be caused by the photosubstitution of CO by 2-MeTHF due to the large difference in their coordinating properties. However, this certainly cannot be the case for the substitution of CO by P(OMe)$_3$, since both CO and P(OMe)$_3$ are π-acceptor ligands which differ little in their coordinating properties. The large spectral shift in the case of [Mn(Br)-{P(OMe)$_3$}(CO)$_2$(^{i}Pr-DAB)] can therefore only be understood if the substitution of CO by P(OMe)$_3$ is accompanied by a change in the halide position from axial to equatorial. Such a site exchange results in a shift of the first absorption band to longer wavelengths [6,17,18]. For example, the fac to mer isomerization of *fac*-[Mn(Br)(CO)$_3$(^{i}Pr-DAB)] is accompanied by a shift of the absorption band from 485 to 590 nm. This shift has recently been rationalized in a density functional molecular orbital study of the fac and mer isomers of [Mn(Cl)(CO)$_3$(bpy)] [17]. A similar effect of the axial-to-equatorial site exchange on the position of the lowest absorption band has recently been observed for the corresponding Me complex *fac*-[Mn(Me)(CO)$_3$(^{i}Pr-DAB)] [18]. It is therefore concluded that the large shift of the absorption band on going from *fac*-[Mn(Br)(CO)$_3$-(^{i}Pr-DAB)] to [Mn(Br){P(OMe)$_3$}(CO)$_2$(^{i}Pr-DAB)] is caused by the combined effect of substitution and site exchange. The same structure is expected for the solvent-substituted photoproduct [Mn(Br)(2-MeTHF)(CO)$_2$(α-diimine)] [6], pointing to the formation of isomer **b** in Scheme 1.

The RT/FTIR technique has enabled a study to be made of the backreaction of the mer complexes to give the fac isomers and the determination of their activation parameters. The calculated lifetime of *mer*-[Mn(Br)(CO)$_3$(^{t}Bu-DAB)] (τ = 1.2 s at 293 K) is short compared with that of the corresponding *mer*-[Mn(Br)(CO)$_3$(^{i}Pr-DAB)] complex (τ = 36.8 s at 293 K). Although their activation enthalpies of thermal isomerization are comparable ($\Delta H^{\ddagger} = 89.1 \pm 6.8$ kJ mol^{-1} for R ≡ ^{i}Pr and $\Delta H^{\ddagger} = 86.5 \pm 1.6$ kJ mol^{-1} for R ≡ ^{t}Bu), the activation entropies are rather different ($\Delta S^{\ddagger} = 29 \pm 24$ J mol^{-1} K^{-1} for R ≡ ^{i}Pr and $\Delta S^{\ddagger} = 49 \pm 6$ J mol^{-1} K^{-1} for R ≡ ^{t}Bu). The large difference in lifetime is thus mainly due to the difference in $\Delta S^{\ddagger}$. A detailed discussion of the influence of the α-diimine and halide ligands, as well as the solvent, on this thermal isomerization will be published in a forthcoming article [19].

5. Conclusions

The above results clearly show that RT/FTIR spectroscopy is a very valuable technique for following thermal reactions and for the detection and identification of intermediates of photochemical reactions at ambient conditions on a timescale of 10^{-1}–10^{1} s. In this respect, the RT/FTIR technique fills the gap between nanosecond to microsecond and conventional IR spectroscopy.

Acknowledgements

We wish to thank H. Luyten, A. Terpstra and Th.L. Snoeck for technical assistance. Thanks are due to the Netherlands Foundation for Chemical Research (SON) and the Netherlands Organization for the Advancement of Pure Research (NWO) for financial support.

References

[1] G.L. Geoffroy and M.S. Wrighton, *Organometallic Photochemistry*, Academic Press, New York, 1979.
[2] T.L. Meyer, *Pure Appl. Chem.*, *58* (1986) 1193.
[3] A.J. Lees, *Chem. Rev.*, *87* (1987) 711.
[4] D.J. Stufkens, *Coord. Chem. Rev.*, *104* (1990) 39.
[5] T.J. Meyer, *Acc. Chem. Res.*, *22* (1989) 163. K.S. Schanze, D.B. MacQueen, T.A. Perkins and L.A. Cabana, *Coord. Chem. Rev.*, *122* (1993) 63. D.J. Stufkens, *Comments Inorg. Chem.*, *13* (1992) 359, and references cited therein.
[6] G.J. Stor, S.L. Morrison, D.J. Stufkens and A. Oskam, *Organometallics*, *13* (1994) 2641.
[7] A. Rosa, G. Ricciardi, E.J. Baerends and D.J. Stufkens, *J. Phys. Chem.*, *100* (1996) 15346.
[8] R.J. Kazlauskas and M.S. Wrighton, *J. Am. Chem. Soc.*, *104* (1982) 5784.
[9] D.P. Drolet, L. Chan and A.J. Lees, *Organometallics*, *7* (1988) 2502.

[10] D.B. Yang, *Appl. Spectrosc.*, *47* (1993) 1425.
[11] H. Bock and H. tom Dieck, *Chem. Ber.*, *100* (1967) 228.
[12] L.H. Staal, A. Oskam and K. Vrieze, *J. Organomet. Chem.*, *170* (1979) 235.
[13] F. Bombin, G.A. Carriedo, J.A. Miguel and J.A. Riera, *J. Chem. Soc., Dalton Trans.*, (1981) 2049. G.A. Carriedo and V. Riera, *J. Organomet. Chem.*, *205* (1981) 371.
[14] A.M. Bond, R. Colton and M.J. McCormick, *Inorg. Chem.*, *16* (1977) 155.
[15] B.D. Rossenaar, F. Hartl, D.J. Stufkens, C. Amatore, E. Maisonhaute and J.N. Verpeaux, *Organometallics*, submitted for publication.
[16] J.J. Turner, M.W. George, F.P.A. Johnson and J.R. Westwell, *Coord. Chem. Rev.*, *125* (1993) 101.
[17] G.J. Stor, D.J. Stufkens, P. Vernooijs, E.J. Baerends, J. Fraanje and K. Goubits, *Inorg. Chem.*, *34* (1995) 1588.
[18] B.D. Rossenaar, A. Oskam, D.J. Stufkens, J. Fraanje and K. Goubitz, *Inorg. Chim. Acta*, *247* (1996) 215.
[19] C.J. Kleverlaan, to be published.